Electrical impedance tomography for simulated muscle contraction: a viability analysis

Luiz Augusto Kalva de Andrade
Programa de Pós Graduação em Bioengenharia
Pontifícia Universiddade Católica do Paraná, Brazil
ORCID: 0000-0002-9571-2056

Mauren Abreu de Souza
Programa de Pós Graduação em Bioengenharia
Pontifícia Universiddade Católica do Paraná, Brazil
ORCID: 0000-0001-6137-918X

Elisangela Ferretti Manffra
Programa de Pós Graduação em Bioengenharia
Pontifícia Universiddade Católica do Paraná, Brazil
ORCID: 0000-0003-1178-0367

Abstract*— Muscles problems could be studied by analysis of their electrical properties. This work realized EIT simulations for muscles under contractions. The EIT images can differentiate muscles positions and sizes by their contractions. Some electrical methods to evaluate the muscle conditions, analyses the muscle as a geometric structure, the bioimpedance analysis (BIA), and other analyses the muscle as a specific part, the electrical impedance myography (EIM). Both methods are already practical methods to evaluate muscles conditions but they don't evaluate muscles as the image techniques, like magnetic resonance and sonography not always accessible. Regarding these techniques an alternative is presented: electrical impedance tomography (EIT). Accessible and well commented for other applications like brain activity imaging, breast imaging, liver fat detection, and bladder volume estimation. The EIT prospects to become an alternative muscle evaluation method alongside BIA and EIM. The forward problem solution method is briefly commented on, also the simulated model construction with your tissues and electrodes. Current patterns usage and the Inverse Problem solution through Electrical Impedance and Diffuse Optical Tomography Reconstruction Software (EIDORS) library. As result, the numerical EIT model permitted EIT images were achieved from different muscles contractions. An EIT model of transfemoral tomography was made, providing some EIT images. Each EIT image was derived from forward problem solutions. Comparisons permitted to conclude the advantages of a more realistic EIT numerical model. A numerical model permits to adapt and reorganize the model easier than a real phantom. Muscle contractions were simulated, even deep muscles were detected through EIT.

Keywords* — *Electrical Impedance Tomography, muscle contraction, simulation, EIDORS.

I. INTRODUCTION

Muscles are complex structures that convert chemical energy into mechanical work. The conversion of chemical energy into mechanical work are associated with the membrane systems of muscle fibers and they have been studied by electro-physiological techniques proper to measure their characteristics [1].

In the case of muscle contraction analysis, Hug commented about the challenges of interpreting EMG (Electromyography) patterns, which is further complicated by factors, such as their variability, their electromechanical delay, and their neuromuscular fatigue [2]. Signal filters can change the interpretation of muscle synergies, including the contraction for more internal muscles. They showed the need for a 40Hz band spectrum, to register other muscles activities in co-contractions. But in many cases, the EMG is restricted for peripheral muscles studies despite its inability to measure deep muscles.

Muscles problems could be resolved through the analysis of electrical properties distributed through the body. Being more specific, these properties of interest are conductivity and permittivity. Electric conductivity relates to the ease with which an electric current flows through the matter. The electric permittivity is a measure of how the charges, of a given material, are reoriented allowing the passage of an alternating electric field. These properties differ among the body tissues [3].

The living tissue structures have different effects to alternating electrical signals applied, resulting in a complex electrical impedance which is called bioelectrical impedance or bioimpedance [4]. This bioimpedance depends on the tissue composition, health status, current directions as well as the frequency of the applied alternate signal. The physiological and physiochemical state of tissue varies with applied signal frequency. Moreover, the bioimpedance dependence on the current direction applied is due to anisotropic structures whose parameters change for different directions considered [5–7].

Bioimpedance analysis (BIA) is one of bioimpedance practical methods to evaluate muscles formation providing a noninvasive test that could be made in a clinic visit [8]. BIA estimates body composition through equations that use different electrical conductivity measures among tissues considered (e.g., bones, adipose, muscle, cartilage). Impedance (resistance and reactance of tissues) is registered using a low current that passes through the body. The different BIA devices use different prediction equations, the number of tactile electrodes, and the frequencies of alternating current.

Other bioimpedance medical test is the electrical impedance myography (EIM), which can provide a quantitative index of muscle condition that help the diagnosis, disease progression trends, and the impact of therapy applied [9]. It can use invasive (needle electrodes) and non-invasive (surface adhesive eletrodes). EIM has been studied for several conditions from amyotrophic lateral sclerosis to muscular dystrophy. When EIM makes the use of adhesive electrodes, they are placed manually on the skin overlying muscle group under analysis and then, it is applied an alternating electrical current which becomes possible a voltage measurement and consequently a bioimpedance determination.

EIM and BIA use the same principle to evaluate the body condition. However, BIA measures a huge segment of the body at once [10]. Because of this, skeletal muscle mass prediction is shared by other tissues, including abdominal fat, bone, gut and bladder contents, and major organs. Also, BIA is strongly impacted by hydration level since electrical currents will always follow the path of minor resistance, usually along conductive fluids contained inner large veins and arteries. Another condition to consider, BIA is based on simplistic volume models which the torso and limbs are simple cylinders, limiting your accuracy and reliability. Apparently, EIM is unaffected by hydration status and, their current flow is less interfered by veins and arteries. When needle electrodes are used instead of surface electrodes, currents are applied directly in the muscle, making them restricted to the muscle avoiding uncertainties of electrode position variations that impact all other forms of BIA [9].

Imaging techniques are available to evaluate body composition and, consequently they can evaluate muscles condition. These techniques are DEXA (Dual X-Ray Absorptiometry), MRI (Magnet Resonance Imaging), CT (Computerized Tomography) and sonography [10]. DEXA measurements of lean and fat mass have widely accepted accuracy and precision that have been validated in multiple clinical environments. Axial CT images can be used as a valid and precise method to estimate whole-body composition. MRI is regarded as the most sophisticated imaging technique for characterizing the loss of muscle mass, as manifested some times by abnormal edema, adipose tissue (myosteatosis), and fibrous connective tissue (myofibrosis). Sonography has been used in several cross-sectional and longitudinal studies to assess muscle conditions through muscle thickness measurements.

Regarding all image methods to measure muscle volumes, MRI and sonography do not make use of ionization beams. However, they are not ever accessible technology. Instead of the hazardous condition of ionizing radiation through the use of a more accessible image method, the Electric Impedance Tomography (EIT) compared to some imaging techniques, has some advantages: noninvasive, radiation-free, non-ionizing method, fast data acquisition, high temporal resolution, medically safe process compared, low-cost device, and suitable for bedside measurement [4].

The EIT is a computed tomographic image reconstruction technique, that uses a specific method to determine internal bioimpedances [4]. Through solving a nonlinear inverse problem in which the biological admittance (or your inverse: the bioimpedance) of a conducting domain is calculated from the surface potentials generated by a current signal injected at the domain boundary (Ω). The result serves to determine the conductive domain to be viewed as an image of conductivities.

Some particularities inherent in EIT need to be overcome as: non-linearity, ill-posed, modeling error, and measurement error. However, EIT systems are developed bringing some particular medical applications like brain activity imaging [11], breast imaging [12], liver fat detection [13], bladder volume estimation [14], prostate imaging [15], hand gestures [16], measuring osteopenia of the pelvis [17], pulmonary evaluation during COVID-19 patients treatment [18] and so on. Regarding these applications, the EIT prospects to become an alternative muscle evaluation method alongside BIA and EIM.

Saline phantoms with some solid inorganic or organic materials are very popular to test EIT circuits and algorithms [4]. However, they cannot mimic with great fidelity the human body regions. Usually, the saline solution is constant in the frequency response, thus this phantom fails to represent a model. The response of the signals in the real organic tissue varies with the frequency and direction of signals applied, their anisotropic behavior explains this [5,6].

Facing these limitations of the saline phantom, a numerical simulated organic model of muscle with real values and properties of organic tissues seems more suitable to test EIT systems and algorithms. Regarding these facts, this article brings a series of numerical simulations to evaluate muscle contractions, even in the deep muscles, through the simulated EIT method.

II. Materials and Methods

II.A. The Forward Problem

The forward EIT problem can be described as the determination of the electric potential distribution in the domain ϕ, which is the region of potential distribution generated by applied current, and represented by the generalized Laplace equation. For a given conductivity distribution σ inside the domain and current density J injected through the boundary [19], the generalized elliptic equation is defined by

$$\nabla\bullet(\sigma\nabla\phi) = 0 \quad (1)$$

with the boundary condition:

$$\sigma(\partial\phi/\partial\check{n}) = J \quad (2)$$

where $\check{n}$ is the a normal vector. In the forward problem calculation, the electrical potential distribution could be calculated from the known current source and tissues electrical properties.

The EIT forward problem reconstruction needs a model capable to source the potentials on specific locations (electrodes) for a given conductivity distribution [20]. The calculated conductivity is adjusted (after the voltages measures) until the calculated voltages fits measurement precision. A series of voltages calculations over the electrodes must be made to achieve a precision better than the accuracy of the measurements.

To generate the simulated potentials of an EIT tomography, we used the COMSOL Multiphysics simulation tool [21]. The simulated voltages were calculated in a forward method, where the current density and the conductivity of biological and non-biological materials were previously determined through values found in the literature for the frequency of 10kHz. The EIT domain was modeled using a magnetic resonance imaging (MRI) image provided by [22] in a previous study of muscle morphology.

A transfemoral image consisting of muscles, nerves, vessels, and other structures was segmented to determine these parts with different conductivities and it can be viewed at Fig. 1. The fat and skin structures do not appear in the segmented image, but in the final model for simulation: fat, skin and electrodes contour were included. Vastus medialis (VM), vastus lateralis (VL), vastus intermedius (VI), rectus femoris (RF), hamstrings (biceps femoris long head (BFlh), biceps femoris short head (BFsh), semitendinosus (ST),

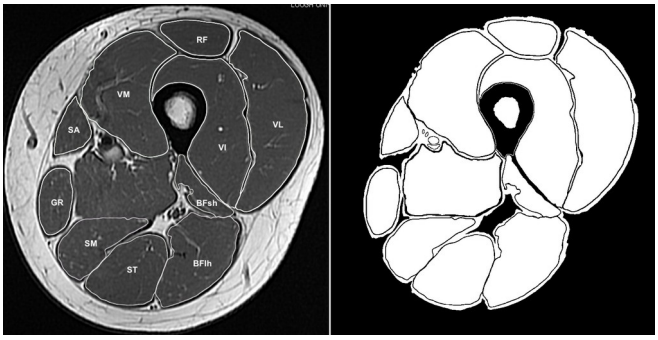

Fig. 1: MRI image and segmented image of transfemoral image of the middle thigh.

semimembranosus (SM)), sartorius (SA) and gracilis (GR) muscles were manually outlined by [22].

Due to compatibility purposes, the segmented image was converted to DXF type archive, the file format used by COMSOL for images. The conversion was through the use of SolidWorks Software [23].

Some tissues conductivity and permittivity values are detailed in Table 1 and they were extracted from [24]. Also, the conductivities and permittivities of muscles under investigation are changed for values in a range considered normal (increase of 15% of impedivitty and 10% relative permittivity compared at rest condition) in invasive *invivo* tests realized by [25], for evaluated muscle contraction.

The COMSOL calculates the simulated potentials of boundary by the Direct method using MUMPS (MUltifrontal Massively Parallel Solver) [26]. This resulting data was used to feed the following EIT inverse problem calculation. The biggest output matrix data to generate had 4096 values, which it contains potential values of all 64 electrodes configuration, including the current electrodes.

II.B.The Finite Element Method

An alternative option to solve partial differential equations (PDEs) is to approximate numerical solutions to solve the numerical model equations. For this, the forward problem can be solved numerically by the finite element method (FEM) through simple shapes that divide the whole domain [27].

For the forward problem, we used a triangular extremely fine mesh in COMSOL, resulting in 554786 elements. The FEM method applied in this simulation is the Weighted Residual Method. The reference was determined at the central point of the model, a potential of 0V, for compatibility purposes with FEM model used for the inverse problem calculation.

TABLE 1: TISSUES CONDUCTIVITIES AND PERMITTIVIES USED IN MODEL

Tissues condutivities and permittivities at 10kHz		
Tissue name	**Conductivity (S/m)**	**Relative Permittivity**
Muscle	0.34083	25909
Muscle contractile	0.29637	28500
Fat	0.02383	1085.3
Nerve	0.042403	35569
Blood	0.70004	5248.2
Blood Vessel	0.31308	7690.8
Bone	0.082623	1657.8
Marrow Bone	0.0027347	675.91
Dry skin	0.00020408	1133.6

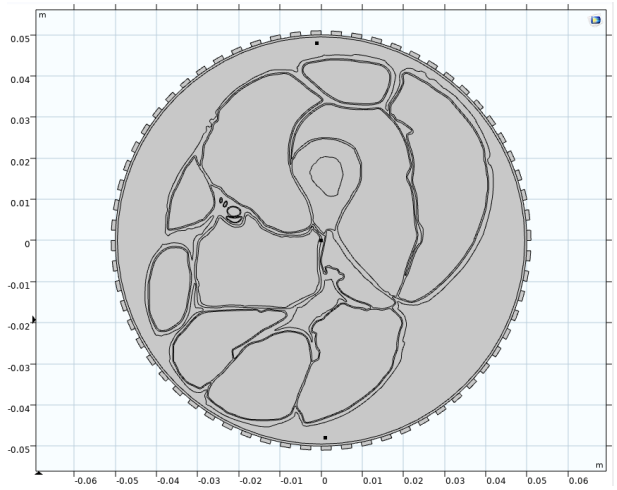
Fig. 2: EIT model with electrodes surrounding the transfemoral region.

In order to guarantee max fidelity with a real EIT image and compatibility with EIDORS, the EIT model brings many aspects to consider: number of tissues, number of electrodes, electrodes positioning, and mesh size. Fig. 2 shows the complete EIT model of transfemoral image with other tissues and structures not present in anterior segmentation but included to increase the simulation reality. The FEM resulting for forward problem generates 1110289 degrees of freedom.

II.C. Current patterns

For determination of conductivities, a current must be injected at specific electrodes of the domain boundary (points of current entrance). Many EIT devices perform current injection through a pair of electrodes, using a called bipolar current source [20]. In this case, we only used an adjacent pattern, which bipolar current passes through pairs of electrodes as Fig.3. A set of measurements is made to create a linearly independent set of measurements, generated by the application and sequential change of current inlet and outlet.

To implement the current patterns tested, it was created an application in COMSOL. This application was capable to commute the currents simulated among electrodes in the model with adjusted current amplitude. For the forward problem solution, the current amplitude was 5mA and the current pattern is adjacent for all images. The solution time takes 20 minutes and 41 seconds to solve all 64 electrodes potentials values for each EIT forward problem generated.

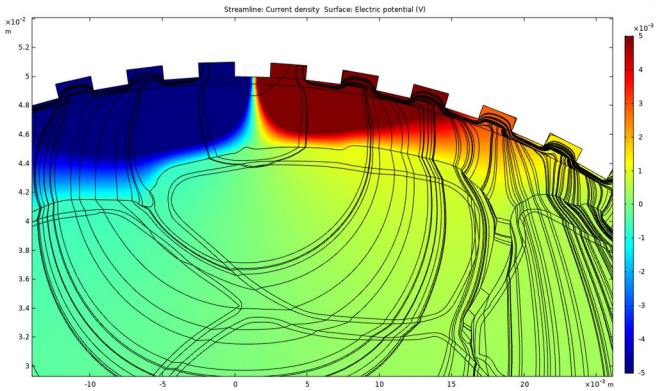

Fig. 3: Potentials generated in an adjacent current applied. Bargraph shows potential variation, and lines of currents between electrodes could be seen.

II.D. The Inverse Problem Solution

The EIT evolves a spatial conductivity determination in an inverse problem, and some methods have similar ways to solve the inverse problem at the iterative process. The beginning is the set of the input or our potential measurements, and this is made for all current and voltage electrodes combinations necessary. A measurement matrix is built, and with its data, is realized a series of tries to reduce the residual error for an initial conductivity estimation. The main process to find the solution is an iterative loop in which a forward problem is evaluated many times, where conductivities are obtained from calculated potentials [20]. Here, instead of *invivo* measurements, the measured potentials are the simulated potentials, and they are continuously compared with calculated potential until the residual error is less than measured potential precision.

For the inverse problem step calculation, we used some previous steps: the FEM and the forward problem calculation. In this step, to evaluate the EIT for muscle evaluation, we generate some MATLAB algorithms [28] with Electrical Impedance and Diffuse Optical Tomography Reconstruction Software (EIDORS) library [29,30] to solve the inverse problem. The EIDORS library has its own FEM models. And to utilize them to build the EIT image, its necessary choose a FEM and adjust it with a number of elements and boundary electrodes. Our chosen model has 64 electrodes with 1024 elements with nodes positioned in a manner that near elements to electrodes are smaller than the electrodes located in the center of the circular domain. Fig. 4 shows how the sizes of elements are disposed inside of the domain.

To investigate a specific muscle in an inverse problem method, it is changed only the observed muscle conductivity and permittivity (considering a contraction), maintaining the other muscles the same rest values. This forward problem reconstruction is compared with another forward problem reconstruction wherein all muscles having the same conductivities and permittivities are not seen, allowing an inverse problem solution by the Newton–Raphson method.

Although the EIDORS does not require that the number of measurements be equal to the number of stimulation patterns (this means that measurement data is not a quadratic matrix), this forward model has quadratic matrix data for future implementation in other reconstruction methods.

II.E.Computation setup

To run the two software (COMSOL and MATLAB) to compute both forward and inverse problems, a notebook with main processor i5-9300H, graphics card model GTX-1650, and 8 Gigabytes of RAM (Random Access Memory) was used to computation work.

III. RESULTS

The EIT images generate are normalized conductivities distribution where an image is constructed by differences in conductivity. Fig. 5 shows the result of EIT inverse problem solution. Individually each muscle was its conductivity altered and this difference of conductance was calculated by the inverse problem solution. A sidebar graph shows a color scale, indicating the conductance change. Muscles in the contracted simulation were VL, VI, Bfsh, ST, Bflh, SM, GR, SA, and VM and they appear in order.

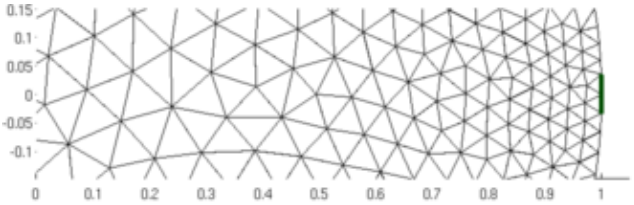

Fig. 4: A part of mesh generated. At right (in green color) it is possible to see the electrode position.

IV. DISCUSSION

The numerical EIT model seems suitable for algorithms test before hardware implementation and *invivo* studies. The EIT application could provide many tests to determine which setup (with current amplitude and patterns) is ideal to apply and to detect conductance differences.

All EIT images generated are derived from two forward solutions: one, when all muscles have the same conductivities, and the other when only one muscle owns its conductivity changed maintaining the other muscles unaltered.

Although, the impedance change do not reflect with precision the muscle area contour (it is viewed by gradual color change from deep blue to bright blue) due to error compensation of inverse problem algorithm, mesh distribution where bigger elements are located near to the domain center, muscle position errors due low conductance of fat around muscles, and number of electrodes.

It is clear that other aggregated methods could enhance the quality image generate. AI (Artificial Intelligence) or statistical algorithms can improve the muscle position and contour precision [31]. And, of course muscles are not in isolated contractions, the simulations here considered the change for one muscle at time.

The images of muscle contractions Bfsh and SA show a lower conductivity differences compared with other muscles positions. The muscles size and the lower currents passing by these muscles could contribute for this lower difference detected.

Some comparisons were made to elucidate some limitations of our model. Table 2 brings this comparison with other models used to simulate EIT images. Griffiths [32] used a wired EIT phantom constructed by resistors mesh, giving some mechanical resistance, and conductance changes were made by putting in parallel another resistor or capacitor. Cheney [3] constructed a phantom in a tank with salty water and agar to simulate different tissues. Real phantoms are good tools to test performance of EIT hardware, but they add-up some uncertainties like noise and temperature variability.

Yorkey [33] employed a numerical model, to compare algorithms to reconstruct images from rectangular domains containing two different conductances. Murphy [34] used a numerical model to simulate a superficial muscle imaging over ultrasound probe, but it does not make a regular EIT. These numerical models do not reflect a realistic *invivo* medium of EIT because of domain geometry and tissues number considered.

TABLE 2: COMPARISON BETWEEN THE DEVELOPED MUSCLE MODEL AND OTHER MODELS FROM THE LITERATURE

Models compared			
Model made by	**Type of Model**	**Number of tissues**	**Number of electrodes**
Griffiths (1998)	Resistor-mesh	2	16
Cheney et al. (1999)	Salt and Agar	3	32
Yorkey et al. (1987)	Numerical	2	16
Murphy et al. (2018)	Numerical	4	16 – 20
Hamilton and Hauptmann (2018)	Numerical and Agar/Graphite	5	16 – 32

Hamilton and Hauptmann [31] used phantoms to validate and numerical models to train their D-Bar with Deep learning algorithms for EIT. They show satisfactory results to use numerical models to train EIT algorithms.

Comparisons with EIT images acquired from a lower number of electrodes are necessary. Normally the EIT systems own a number of 16 or 32 electrodes to acquire the potentials, talking about the electronic project, this means use existent commercial multiplexers to construct. Maybe a 32 electrode EIT model with smaller matrices, could bring very similar results as 64 electrodes. This is a question to elucidate. Other posterior works can include different frequencies of current applied, muscles in group contractions, and simulated uncertainties.

V. CONCLUSION

A numerical model for EIT containing many tissues and geometry was made, and it is compatible with the FEM model, used to solve the inverse problem. A numerical model permits adaptation and reorganizes the model easier than a real phantom. Muscle contractions were simulated, even deep muscles were detected through EIT.

CONFLICT OF INTEREST STATEMENT

On behalf of all authors, the corresponding author states that there is no conflict of interest.

ACKNOWLEDGMENT

This study was financed in part by the Coordenação de Aperfeiçoamento de Pessoal de Nível Superior - Brasil (CAPES)- Finance Code 001.

REFERENCES

1. Eisenberg RS. Impedance Measurement of the Electrical Structure of Skeletal Muscle. Compr Physiol. 1983;(May):301–23.
2. Hug F. Can muscle coordination be precisely studied by surface electromyography? J Electromyogr Kinesiol. 2011;21(1):1–12.
3. Cheney M, Isaacson D, Jonathan C. Newell. Electrical impedance tomography. Med Imaging Princ Pract. 2012;41(1):7-18-8–25.
4. Bera TK. Bioelectrical Impedance Methods for Noninvasive Health Monitoring: A Review. J Med Eng. 2014;2014:1–28.
5. Epstein BR, Foster KR. Anisotropy in the dielectric properties of skeletal muscle. Med Biol Eng Comput. 1983;21(1):51–5.
6. Aaron R, Huang M, Shiffman CA. Anisotropy of human muscle via non-invasive impedance measurements. Phys Med Biol. 1997;42(7):1245–62.
7. Kashuri H. Anisotropy of human muscle via non invasive impedance measurements . Frequency dependence of the impedance changes during isometric. 2008;1–125.
8. Aleixo GFP, Shachar SS, Nyrop KA, Muss HB, Battaglini CL, Williams GR. Bioelectrical Impedance Analysis for the Assessment of Sarcopenia in Patients with Cancer: A Systematic Review. Oncologist. 2020;25(2):170–82.
9. Clark BC, Rutkove S, Lupton EC, Padilla CJ, Arnold WD. Potential Utility of Electrical Impedance Myography in Evaluating Age-Related Skeletal Muscle Function Deficits. Front Physiol. 2021;12(May).
10. Boutin RD, Yao L, Canter RJ, Lenchik L. Sarcopenia: Current concepts and imaging implications. Am J Roentgenol. 2015;205(3):W255–66.

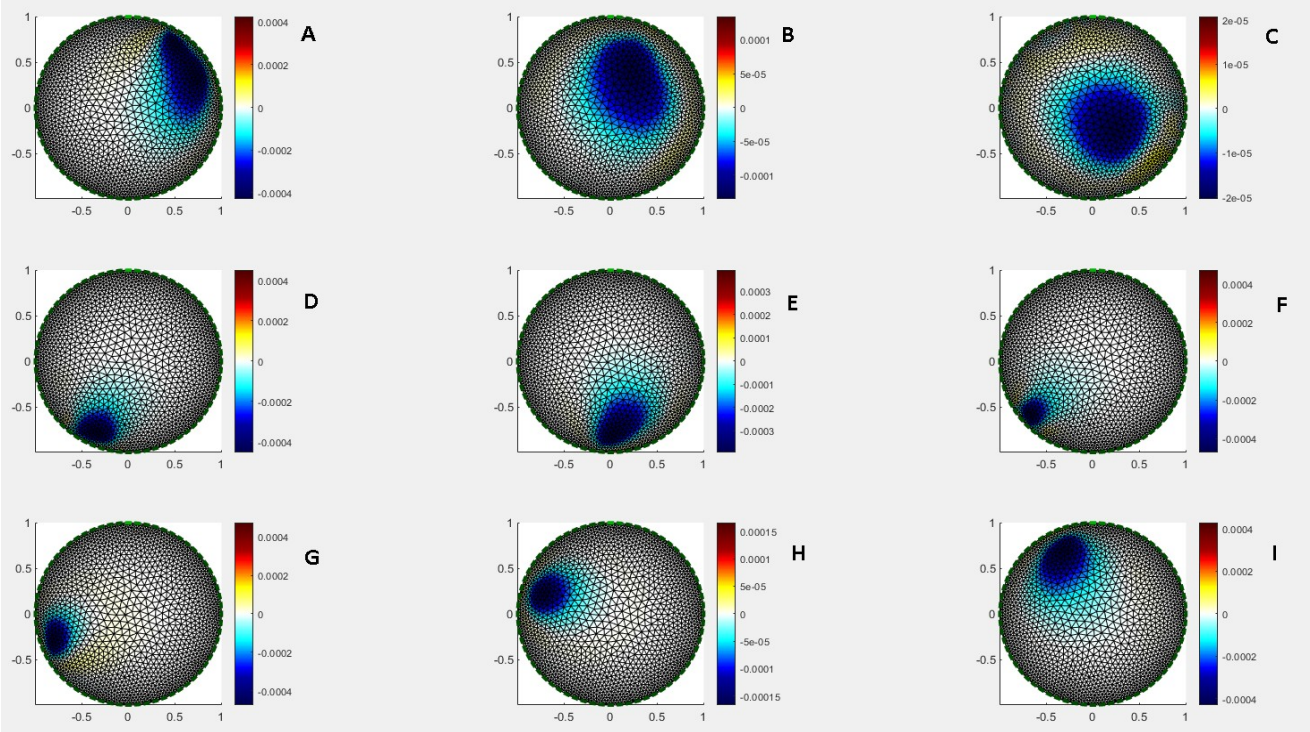

Fig. 5: The EIT results from muscles contractions at 10kHz current frequency. Muscle contractions were simulated followed by letters: VL - A, VI - B, Bfsh - C, ST - D, Bflh - E, SM - F, GR - G, SA - H, and VM - I. Side bargraphs shows the conductance in variation scale.

11. Aristovich KY, Packham BC, Koo H, Santos GS dos, McEvoy A, Holder DS. Imaging fast electrical activity in the brain with electrical impedance tomography. Neuroimage [Internet]. 2016;124:204–13. Available from: http://dx.doi.org/10.1016/j.neuroimage.2015.08.071
12. Prasad SN, Houserkova D, Campbell J. Breast imaging using 3D electrical impedence tomography. Biomed Pap Med Fac Univ Palacky Olomouc Czech Repub. 2008;152(1):151–4.
13. Chang C-C, Huang Z-Y, Shih S-F, Luo Y, Ko A, Cui Q, et al. Liver electrical impedance tomography for early identification of fatty infiltrate in obesity. bioRxiv. 2020;
14. Schlebusch T, Nienke S, Leonhardt S, Walter M. Bladder volume estimation from electrical impedance tomography. Physiol Meas. 2014;35(9):1813–23.
15. Rao A, Murphy EK, Halter RJ, Odame KM. A 1 MHz Miniaturized Electrical Impedance Tomography System for Prostate Imaging. IEEE Trans Biomed Circuits Syst. 2020;14(4):787–99.
16. Zhang Y, Xiao R, Harrison C. Advancing hand gesture recognition with high resolution electrical impedance tomography. UIST 2016 - Proc 29th Annu Symp User Interface Softw Technol. 2016;843–50.
17. Kimel-Naor S, Abboud S, Arad M. Parametric electrical impedance tomography for measuring bone mineral density in the pelvis using a computational model. Med Eng Phys [Internet]. 2016;38(8):701–7. Available from: http://dx.doi.org/10.1016/j.medengphy.2016.04.013
18. Van Der Zee P, Somhorst P, Endeman H, Gommers D. Electrical impedance tomography for positive end-expiratory pressure titration in COVID-19-related acute respiratory distress syndrome. Am J Respir Crit Care Med. 2020;202(2):280–4.
19. Lionheart WRB. EIT reconstruction algorithms: Pitfalls, challenges and recent developments. Physiol Meas. 2004;25(1):125–42.
20. Martins T de C, Sato AK, de Moura FS, de Camargo EDLB, Silva OL, Santos TBR, et al. A review of electrical impedance tomography in lung applications: Theory and algorithms for absolute images. Annu Rev Control. 2019;48(xxxx):442–71.
21. COMSOL. COMSOL MULTIPHYSICS [Internet]. 2020 [cited 2020 Jun 22]. Available from: https://www.comsol.com/comsol-multiphysics
22. Behan FP, Maden-Wilkinson TM, Pain MTG, Folland JP. Sex differences in muscle morphology of the knee flexors and knee extensors. PLoS One. 2018;13(1).
23. Solidworks. Solidworks CAD [Internet]. 2020 [cited 2020 Mar 8]. Available from: https://www.solidworks.com/
24. Gabriel C, Gabriel S, Corthout E. The dielectric properties of biological tissues: I. Literature survey. Phys Med Biol. 1996;41(11):2231–49.
25. Coutinho ABB, Jotta B, Werneck-De-Castro JP, Pino A V., Souza MN. Invasive electrical impedance myography at different levels of contraction of gastrocnemius muscle of rat. Rev Sci Instrum [Internet]. 2020;91(8). Available from: https://doi.org/10.1063/1.5131631
26. MUMPS. MUMPS - MUltifrontal Massively Parallel Solver. 2011;1–54.
27. Jafarpoor M, Li J, White JK, Rutkove SB. Optimizing electrode configuration for electrical impedance measurements of muscle via the finite element method. IEEE Trans Biomed Eng. 2013;60(5):1446–52.
28. MATLAB. MATLAB [Internet]. 2021 [cited 2021 Dec 8]. Available from: https://www.mathworks.com/products/matlab.html
29. Polydorides N, Lionheart WRB. A Matlab toolkit for three-dimensional electrical impedance tomography: A contribution to the Electrical Impedance and Diffuse Optical Reconstruction Software project. Meas Sci Technol. 2002;13(12):1871–83.
30. Adler A, Lionheart WRB. Uses and abuses of EIDORS: An extensible software base for EIT. Physiol Meas. 2006;27(5).
31. Hamilton SJ, Hauptmann A. Deep D-Bar: Real-Time Electrical Impedance Tomography Imaging With Deep Neural Networks. IEEE Trans Med Imaging. 2018;37(10):2367–77.
32. Griffiths H. A phantom for electrical impedance tomography. Clin Phys Physiol Meas. 1988;9(4A):15–20.
33. Yorkey TJ, Webster JG, Tompkins WJ. Algorthms for Impedance Tomography Electrcal. Technology. 1987;(11):843–52.
34. Murphy EK, Skinner J, Martucci M, Rutkove SB, Halter RJ. Toward Electrical Impedance Tomography Coupled Ultrasound Imaging for Assessing Muscle Health. IEEE Trans Med Imaging. 2019;38(6):1409–19.